

# Comparing Elementary Cellular Automata Classifications with a Convolutional Neural Network

Thibaud Comelli<sup>1</sup>, Frédéric Pinel<sup>2</sup> and Pascal Bouvry<sup>2</sup>

<sup>1</sup>Polytech Lille, University of Lille, France

<sup>2</sup>Faculty of Science, Technology and Medicine, University of Luxembourg, Luxembourg

**Keywords:** Cellular Automata, Cellular Automata Classification, Convolutional Neural Network.

**Abstract:** Elementary cellular automata (ECA) are simple dynamic systems which display complex behaviour from simple local interactions. The complex behaviour is apparent in the two-dimensional temporal evolution of a cellular automata, which can be viewed as an image composed of black and white pixels. The visual patterns within these images inspired several ECA classifications, aimed at matching the automatas' properties to observed patterns, visual or statistical. In this paper, we quantitatively compare 11 ECA classifications. In contrast to the *a priori* logic behind a classification, we propose an *a posteriori* evaluation of a classification. The evaluation employs a convolutional neural network, trained to classify each ECA to its assigned class in a classification. The prediction accuracy indicates how well the convolutional neural network is able to learn the underlying classification logic, and reflects how well this classification logic clusters patterns in the temporal evolution. Results show different prediction accuracy (yet all above 85%), three classifications are very well captured by our simple convolutional neural network (accuracy above 99%), although trained on a small extract from the temporal evolution, and with little observations (100 per ECA, evolving 513 cells). In addition, we explain an unreported "pathological" behaviour in two ECAs.

## 1 INTRODUCTION

This paper reports our findings when comparing existing classifications of elementary cellular automata (ECA) from the perspective of a convolutional neural network (CNN). We will introduce in the next paragraphs ECAs and their classifications, but as a first approximation, we can say that the representation of a cellular automata's temporal evolution (for example: Figure 1) forms an image, which reveals patterns that inspired several researchers to classify the different ECAs under a few classes of behaviour. Figure 2 shows temporal evolutions of three ECAs belonging to different classes in an early and well-known classification (Wolfram, 1984).

The different published ECA classifications are like definitions: their underlying logic is their sole justification, there is no *a posteriori* validation. We propose to quantitatively compare these classifications, thus, we need a comparison method. The image representation of the ECA's temporal evolution suggests the use of convolutional neural networks (CNN) as a judge, this is further explained in Section 2. Next, we introduce the various concepts used in this paper.

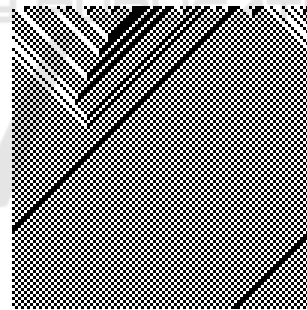


Figure 1: Rule 184 (Bach, 2020).

**Elementary Cellular Automata.** A cellular automata (Von Neumann et al., 1951; Moore and Burks, 1970; Wolfram, 1984) (CA) is the application of one Boolean function, called the CA rule, which maps the next value of a cell, from its previous value and its neighbours' values. The rule is individually applied to an array of cells, also called a configuration. While the rule defines the behaviour of a CA, additional information is needed to fully execute a CA. Here, we are concerned with elementary cellular automata: one-dimensional (the configuration is one-dimensional), each cell takes the value 0 or 1 (white

or black), the rule's domain are three cells, the central cell and its left and right neighbours. Additional information is further required to fully compute the evolution of a CA, the full definition is presented in Section 4.1. As an example, rule 30's truth table is presented below:

■ ■ ■ $\mapsto$ □ = 0	□ ■ ■ $\mapsto$ ■ = 1
■ ■ □ $\mapsto$ □ = 0	□ ■ □ $\mapsto$ ■ = 1
■ □ ■ $\mapsto$ □ = 0	□ □ ■ $\mapsto$ ■ = 1
■ □ □ $\mapsto$ ■ = 1	□ □ □ $\mapsto$ □ = 0

The decimal representation of the mapped values is used to name the rule:  $00011110_2 = 30_{10}$  in this case. The image representation of the temporal evolution is obtained by placing the next value of each cell in the cell array below its previous value.

**Classification.** The simplicity of the ECA is misleading, as its simple local interactions can generate complex behaviours or patterns. Because of this, some authors write (Wuensche et al., 1992) "cellular automata are for complex systems theorists what E. coli are for the biologist: a system simple enough to manipulate experimentally, but complex enough to suggest insights for real-world problems." Some ECAs are shown to be capable of universal computation (Cook, 2004). In addition, ECA behaviours can be clustered, or classified, according to the similar patterns their evolution reveals. This has led to several classifications of ECA behaviour. Wolfram's classification (Wolfram, 1984) defines 4 classes, class I for ECA that converge to uniform configurations, class II when converging to periodic configurations, class III for generating apparent random configurations and class IV for complex configurations, mostly random but with pattern formation. Figure 2 highlights three of those classes, the first (leftmost) rule is considered periodic, the second chaotic and the last (rightmost) complex (Wolfram, 1984; Berto and Tagliabue, 2017). It was also noted that some ECA display different behaviours depending on their initial configuration.

In contrast, other classifications have sought quantitative tools to form classes, instead of the more visual pattern recognition. Wuensche et al. (Wuensche et al., 1992) have further examined the Wolfram classification with basins of attraction fields. Normal Compression (Zenil and Villarreal-Zapata, 2013) base their classification on Kolmogorov complexity (approximated with a lossless compression ratio) and a probabilistic complexity measure, *black entropy* (Wolfram, 2002). Surface Dynamics (Seck Tuoh Mora et al., 2014) rely on statistics, density and

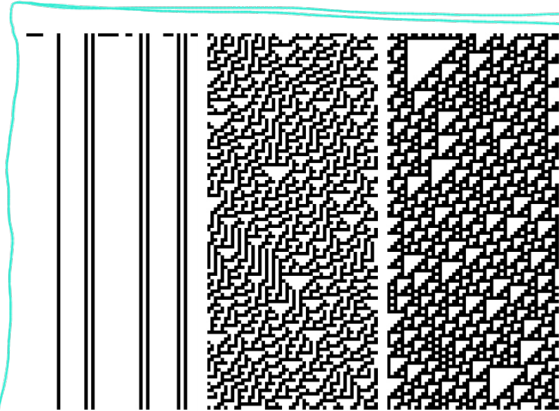


Figure 2: Rules 4, 30 and 110 (Berto and Tagliabue, 2017).

binary values (to further split equal density configurations), predicted with nearest-neighbour interpolation. The statistical model is then used to capture long term effects.

**Convolutional Neural Networks.** The hypothesis behind the choice of the convolutional neural network as the comparison method is that if human pattern recognition or statistical measures inspired the design of a CA classification, then a CNN should also be capable of learning it. Section 4 shows if this hypothesis holds.

To summarize, we aim to compare how well the previously published ECA classifications capture the temporal patterns of the ECA across different configurations. A convolutional neural network is trained for each ECA classification, and its predictive accuracy (of the expected class under that classification) on different ECA configurations is then used to compare the ECA classifications.

## 2 PROPOSED APPROACH

Over time, multiple classifications for ECAs have been proposed. Martínez (Martínez, 2013) provides an exhaustive summary.

In this paper, we propose to quantitatively compare the different ECA classifications through the lens of a neural network: how well can a neural network learn the logic behind an ECA classification. To this end, we will define the input data, a neural network architecture, training and test data sets. The classes defined by each classification represent the expected output, to be predicted by the CNN.

Most ECA classifications derive from the analysis of the two-dimensional representation of the temporal evolution of an ECA, as we saw from Figure 2. Therefore, the chosen neural architecture is

the convolutional neural network (LeCun et al., 1995) (CNN), which has demonstrated its capability for pattern recognition in images (Krizhevsky et al., 2012; Russakovsky et al., 2015), matching and often exceeding human ability (He et al., 2015). The input data to training and testing of the CNN are images: black and white pixels of predetermined fixed size, extracted from the representation of the temporal evolution of an ECA. The executions start from a random initial configuration, which permits the generation of as much data as needed, for training and testing. A common CNN architecture will be trained on each of the ECA classification, then tested for prediction accuracy on unseen ECA executions (from a different initial configuration).

Each classification will then be judged on how accurate the corresponding CNN can predict this classification's classes: how does it grasp the concept underlying that particular classification. We will analyse these results and expose distinctive characteristics of these classifications when possible.

### 3 RELATED WORK

To our best knowledge, there is no previous work comparing ECA classifications. Therefore there is no such comparison based on CNN either, nevertheless, casting the comparison as an instance of the image classification problem suggests the use of a CNN, given its demonstrated capability (see references in Section 2).

Related work includes the proposal of new classification, based or not on previous classification, but relies on a new indicator: a new observed behaviour. Wuensche et al. (Wuensche et al., 1992) have established the concept of *equivalence* classes between CA. He used the left/right and black/white symmetries and has shown that they follow the same behaviour, and therefore should not be assigned to different classes in a classification (equivalent rules are enumerated in (Martínez, 2013)). Langton (Langton, 1990) introduces an indicator  $\lambda$  called *activity*. This represents the ratio of the number of transformation in the rule that lead to a quiescent state. This number has shown to be correlated with Wolfram's classification (Wolfram, 1984). Others, such as Blinder and Oliveira (Binder, 1993) suggest a better analysis of CA behaviour by defining *sensitivity*, *absolute activity*, *neighbourhood dominance* and *activity propagation* (Oliveira et al., 2001b; Oliveira et al., 2001a; de Oliveira et al., 2000). In our work, the CNN is not used as an indicator, or discriminator, that leads to a new classification, rather we employ a CNN as

a observer to determine which of those classifications produce more accurate predictions.

Some previous works make use of neural networks, not for comparison but to automatically classify CAs within a specific classification. Kunkle (Kunkle, 2003) justifies seven parameters used as input data to a neural network. The neural network returns the class in Li and Packard's classification (Li and Packard, 1990) where the rule should belong. The author aims to show the impact of those parameters, however dismissing the visual and random aspect that inspired Wolfram's classification (Wolfram, 1984). Although multiple behaviours of the CA have been described, it says nothing of the capability of alternatives neural networks, such as CNN. Also, the neural network is used to predict a class within a classification, and not to compare classifications, as presented here.

Silverman (Silverman, 2019) used a CNN as a proof of accuracy: his goal was to study ECAs of class IV in Wolfram's classification, ECAs of this class being difficult to categorise. He used a CNN directly on the temporal evolution of cellular automata, as in our paper. After training, the CNN was able to predict the class IV more than 90% even on some higher-complexity spaces. However, Silverman makes no mention of CNN to compare classifications, which is the goal of our paper.

### 4 RESULTS

We begin this section with the experimental setup, Section 4.1, followed by the complete description of an unexpected behaviour for two specific ECAs, Section 4.2. Finally, all results and noteworthy findings are presented in Section 4.3.

We compare 11 known elementary CA classifications: Wolfram, Li and Packard, Wuensche, ECAM, Index complexity, Communication complexity, Topological, Topological dynamics, Normalised compression, Surface dynamics, Spectral. These classifications were gathered in a survey paper by Martínez (Martínez, 2013). However some minor errors remain in that survey paper, so we recommend referring back to the cited reference for each individual classification to avoid mis-classifications.

As mentioned, a CNN will be trained for each classification. All CNNs share the same architecture and will be trained and tested on the same data<sup>1</sup>, where only the class each ECA belongs to varies from one classification to another. Note that the number

<sup>1</sup>Training and test data are different.



of classes also varies per classification (but remains low). The data is composed of the temporal evolution of a CA, starting from a randomly generated initial configuration. More details are found in Section 4.1. After training the CNN for each CA in each classification, we observe the classification errors on the test data set, which serves as the basis for the comparison among different classifications. Additionally, the predicted classes for each CA in each classification is recorded for further analysis (the raw data is not included in the paper).

#### 4.1 Detailed Setup

The CNN is defined by its structure and the training data. The training data is generated as follows. We generate 100 ECA temporal evolutions for each of the 256 ECAs (there are only 256 ECAs, as can be deducted from Section 1). Each ECA evolves an initial configuration of  $512+1$  cells, the configuration is *cyclic* (Wolfram, 2002) (the right neighbor of the rightmost cell is the leftmost cell, and vice versa). Cyclic configurations are sometimes called *wrapped around* (Wuensche et al., 1992).

The ECA iterations start from a random initial configuration, and each new configuration produced in an iteration is represented immediately below the previous configuration values, to form a 2D representation (for example, Figure 1). After 512 iterations, a fixed  $32 \times 32$  area is selected, and the cells' values serve as the input image to the CNN. Other classifications have also relied on a small cell area (Wuensche et al., 1992; Seck Tuoh Mora et al., 2014; Zenil and Villarreal-Zapata, 2013). The different random initial configurations aim to capture the ECA average behaviour (Zenil and Villarreal-Zapata, 2013).

A cyclic configuration produces interference faster (half the iterations) than without. We opted to include the full behaviour of the CA, with interference. Alternatives are: a fixed value (either 0 or 1) at the edges of the array, or a random value. The array length is 513 cells. The typical  $512 = 2^9$  was initially considered, however initial executions showed that rules 60, 90 and their equivalent are nilpotent<sup>2</sup> from random initial configurations, despite Wolfram, Li and Packard classifying them as chaotic. A proof sketch is provided below, Section 4.2, for configurations of  $2^k$  cells.

The CNNs trained for each classification share the same architecture. The chosen architecture is a straightforward sequential model of only 6 layers with an input of a  $32 \times 32$  binary type:

1.  $3 \times 3$  convolution 2D layer,

<sup>2</sup>Configuration cells are all 0 or 1 after several iterations.

2.  $2 \times 2$  max pooling layer,
3.  $3 \times 3$  convolution 2D layer,
4. input flattening layer,
5. 64 dense layer<sup>3</sup>
6. dense layer, where the number of nodes matches the number of classes in the classification being fit.

The activation function is the ReLU, and the optimizer algorithm is Adam. The only difference between CNNs trained for different classifications is the class in the classification each rule belongs to. The same ECA executions (starting from the same random initial configuration) are used across the different classifications.

We have deliberately opted for a simple CNN. Deeper architectures are of course possible, and trainable with the large amount of data that can be generated. Adding convolution layers could capture more elaborate pattern classifications. Also, by considering the ECA rule as *spatial* pattern, operating on a configuration (at one iteration, or one time step), and considering the cells' interference as a *temporal* pattern, we could decompose the CNN into two components, where first a representation of the ECA rule would be inferred from the ECA output, then followed by a rule representation-to-class classifier. The size of the extracted data from the ECA's output would guide the length of the second classifier, while the first is dictated by the number of possible rules (256 for ECA) and the feature extraction of the convolution layers. Such CNN designs would be much larger than the one chosen above, which, as we shall discuss in Section 4.3, achieves significant accuracy.

The testing data is of the same type as the training data, but contains 200 unseen  $32 \times 32$  images for each of the 256 rules, for a total of 51,200 observations.

#### 4.2 Nilpotency of Rules 90 and 60

In this section we propose a proof of the 'pathological' behaviour of two ECA, under specific configuration. The behaviour is that rules 60 and 90 have a nilpotency behaviour when they operate from an cyclic configuration of  $2^k$  cells. The proof also applies to the equivalents of rule 60 (rules 102, 153, 195) and rule 90 (rule 165) (Martínez, 2013).

##### 4.2.1 Notation

The following notation is used in the proof:

<sup>3</sup>Fully-connected layer.

- Symbols  $\square$  and  $\blacksquare$  describe the value of a cell, respectively white (0) and black (1).
- Variables  $x, y$  and  $z$  describe the variable value of a specific cell.
- $C_k$  represents any configuration of  $2^k - 1$  cells, whose exact values are ignored in the reasoning.

We define the operator  $\Rightarrow^i$  between a sub-array of  $k + 2 * i$  cells and a sub-array of  $k$  cells to represent the transformation which defines the  $k$  values of the  $k$  cells. The  $i$  in  $\Rightarrow^i$  indicates the number or CA iterations. These  $k$  values that can be fully determined, despite ignoring other cells to the left or right of the input (left-hand side) sub-array. This explains the smaller output sub-array. The intent is to identify the fully known values after the CA iterations. The configuration on the right-hand side of  $\Rightarrow^i$  leads to the value of the central cell after  $i$  iterations. For example, for rule 90:

$$\square\square\square \Rightarrow^1 \square$$

and

$$\square\blacksquare\square\square\square\square \Rightarrow^2 \square\blacksquare\square \Rightarrow^1 \square$$

#### 4.2.2 Rule 90

Rule 90 implements the Boolean XOR operator on the left and right neighbour. We can express rule 90 with our introduced operator  $\Rightarrow^1$ :

$$xyz \Rightarrow^1 \begin{cases} \square & \text{if } x = z \\ \blacksquare & \text{otherwise} \end{cases}$$

We start with a proof by induction, on  $k \geq 1$ , that:

$$xC_ky \Rightarrow^{2^{k-1}} \begin{cases} \square & \text{if } x = y \\ \blacksquare & \text{otherwise} \end{cases} \quad (1)$$

For the initial case,  $k = 1$ : by definition,  $C_k$  consists of one cell, and according to the definition of rule 90, the inductive hypothesis holds for  $k = 1$ .

Let's assume (1) holds for some  $k \geq 1$ . For the inductive step,  $k + 1$ , we start by establishing the following:

$$\begin{aligned} \square C_k \square C_k \square &\Rightarrow^{2^{k-1}} \square C_k \square \Rightarrow^{2^{k-1}} \square \\ \square C_k \square C_k \blacksquare &\Rightarrow^{2^{k-1}} \square C_k \blacksquare \Rightarrow^{2^{k-1}} \blacksquare \\ \square C_k \blacksquare C_k \square &\Rightarrow^{2^{k-1}} \blacksquare C_k \blacksquare \Rightarrow^{2^{k-1}} \blacksquare \\ \square C_k \blacksquare C_k \blacksquare &\Rightarrow^{2^{k-1}} \blacksquare C_k \square \Rightarrow^{2^{k-1}} \blacksquare \\ \blacksquare C_k \square C_k \square &\Rightarrow^{2^{k-1}} \blacksquare C_k \square \Rightarrow^{2^{k-1}} \blacksquare \\ \blacksquare C_k \square C_k \blacksquare &\Rightarrow^{2^{k-1}} \blacksquare C_k \blacksquare \Rightarrow^{2^{k-1}} \square \\ \blacksquare C_k \blacksquare C_k \square &\Rightarrow^{2^{k-1}} \square C_k \blacksquare \Rightarrow^{2^{k-1}} \blacksquare \\ \blacksquare C_k \blacksquare C_k \blacksquare &\Rightarrow^{2^{k-1}} \square C_k \square \Rightarrow^{2^{k-1}} \square \end{aligned}$$

$C_kxC_k$  consists of  $2^{k+1} - 1$  cells, and from the above expressions, it can be rewritten as:

$$xC_{k+1}y \Rightarrow^{2^k} \begin{cases} \square & \text{if } x = y \\ \blacksquare & \text{otherwise} \end{cases}$$

Thus (1) is proved.

By definition of  $C_k$ ,  $x$  and  $y$  in  $xC_ky$  are separated by  $2^k - 1$  cells. So in the specific case of a  $2^k$  cyclic array the rightmost ( $y$ ) and leftmost neighbour ( $x$ ) point to the same cell. From (1), after  $2^{k-1}$  iterations, each cell transitions to white and, by definition of rule 90, will remain white.

#### 4.2.3 Rule 60

Rule 60 is similar to rule 90: it implements the Boolean XOR operator on the left and center cells. We can also express it with the operator  $\Rightarrow^1$  introduced in Section 4.2.1:

$$xyz \Rightarrow^1 \begin{cases} \square & \text{if } x = y \\ \blacksquare & \text{otherwise} \end{cases}$$

We proceed as for rule 90 with the proof, by induction on  $k \geq 1$ , that:

$$xC_kyC_kC_1 \Rightarrow^{2^k} \begin{cases} \square & \text{if } x = y \\ \blacksquare & \text{otherwise} \end{cases} \quad (2)$$

To discharge the initial case,  $k = 1$ , we observe that:

$$\begin{aligned} \square\square\square xy &\Rightarrow^1 \square\square C_1 \Rightarrow^1 \square \\ \square\square\blacksquare xy &\Rightarrow^1 \square\blacksquare C_1 \Rightarrow^1 \blacksquare \\ \square\blacksquare\square xy &\Rightarrow^1 \blacksquare\blacksquare C_1 \Rightarrow^1 \square \\ \square\blacksquare\blacksquare xy &\Rightarrow^1 \blacksquare\square C_1 \Rightarrow^1 \blacksquare \\ \blacksquare\square\square xy &\Rightarrow^1 \blacksquare\square C_1 \Rightarrow^1 \blacksquare \\ \blacksquare\square\blacksquare xy &\Rightarrow^1 \blacksquare\blacksquare C_1 \Rightarrow^1 \square \\ \blacksquare\blacksquare\square xy &\Rightarrow^1 \square\blacksquare C_1 \Rightarrow^1 \blacksquare \\ \blacksquare\blacksquare\blacksquare xy &\Rightarrow^1 \square\square C_1 \Rightarrow^1 \square \end{aligned}$$

These expressions are of the form:

$$xC_1yC_1C_1 \Rightarrow^{2^1} \begin{cases} \square & \text{if } x = y \\ \blacksquare & \text{otherwise} \end{cases}$$

So the inductive hypothesis holds for  $k = 1$ .

Let's assume (2) holds for some  $k \geq 1$ . For the inductive step,  $k + 1$ , we start by establishing the following:

$$\begin{aligned} \square C_k \square C_k \square C_k x C_k y &\Rightarrow^{2^k} \square C_k \square C_k C_1 \Rightarrow^{2^k} \square \\ \square C_k \square C_k \blacksquare C_k x C_k y &\Rightarrow^{2^k} \square C_k \blacksquare C_k C_1 \Rightarrow^{2^k} \blacksquare \\ \square C_k \blacksquare C_k \square C_k x C_k y &\Rightarrow^{2^k} \blacksquare C_k \blacksquare C_k C_1 \Rightarrow^{2^k} \square \\ \square C_k \blacksquare C_k \blacksquare C_k x C_k y &\Rightarrow^{2^k} \blacksquare C_k \square C_k C_1 \Rightarrow^{2^k} \blacksquare \end{aligned}$$

$$\begin{aligned}
\blacksquare C_k \square C_k \square C_k x C_k y &\Rightarrow^{2^k} \blacksquare C_k \square C_k C_1 \Rightarrow^{2^k} \blacksquare \\
\blacksquare C_k \square C_k \blacksquare C_k x C_k y &\Rightarrow^{2^k} \blacksquare C_k \blacksquare C_k C_1 \Rightarrow^{2^k} \square \\
\blacksquare C_k \blacksquare C_k \square C_k x C_k y &\Rightarrow^{2^k} \square C_k \blacksquare C_k C_1 \Rightarrow^{2^k} \blacksquare \\
\blacksquare C_k \blacksquare C_k \blacksquare C_k x C_k y &\Rightarrow^{2^k} \square C_k \square C_k C_1 \Rightarrow^{2^k} \square
\end{aligned}$$

These expressions are of the form:

$$x C_{k+1} y C_{k+1} C_1 \Rightarrow^{2^{k+1}} \begin{cases} \square & \text{if } x = y \\ \blacksquare & \text{otherwise} \end{cases}$$

Thus (2) has been proved.

By definition of  $C_k$ ,  $x$  and  $y$  in  $x C_k y C_k C_1$  are separated by  $2^k - 1$  cells. So in the specific case of a  $2^k$  cyclic array the rightmost ( $x$ ) and the center cell ( $y$ ) point to the same cell. From (2), after  $2^k$  iterations, each cell transitions to white and, by definition of rule 60, will remain white.

### 4.3 Results and Analysis

As described in the setup, Section 4.1, once a CNN classifier is trained for a classification, it is evaluated on a test set (which counts 51,200 observations, or twice the training data size). Table 1 lists the observed accuracy, for each classification, of the trained CNN classifier (a classification accuracy greater than 99% is typeset in bold).

**Table 1:** Accuracy of the CA rule classifiers (CNN), per classification (on test set).

Classification	CNN accuracy (%)
<b>Wolfram</b>	<b>99.54</b>
Li & Packard	97.58
Wuensche	89.01
ECAM	92.38
Index complexity	87.81
Communication complexity	85.67
<b>Topological</b>	<b>99.08</b>
Topological dynamics	91.99
<b>Normalised compression</b>	<b>99.23</b>
<b>Surface dynamics</b>	<b>99.59</b>
Spectral	96.12

Classifications such as Wolfram's, Surface dynamics and Normalised Compression seem to be well learned by the simple CNN proposed. For reference, they propose 4, 2 and 3 classes respectively. On the other hand, classifications such as Wuensche, Index complexity and Communication complexity are less well learned. They all have 3 classes. Nevertheless, every classification achieves an accuracy of 85% or greater.

The prediction results on the test set reveal more than the overall accuracy for each classification, the results also record the accuracy of each rule, under

each classification. For certain classifications, the images extracted from the temporal evolution of a particular ECA are never classified correctly. In those cases, the CNN classifies most of the 200 unseen ECA execution images in the same incorrect class. The CNN seems to have identified a different pattern from the classification logic. This can depend on our choice of the image extracted from the execution trace.

Under Wolfram's classification, 253 of 256 rules are correctly predicted more than 90% of the time. The least correctly classified rules are rule 104 (68%) and 233 (75.5%). They are considered by Wuensche as equivalent rules, due to their black/white symmetry. Therefore there is some consistency in the CNN predictions. In Wolfram's classification, these rules are labeled class II (periodic behaviour). When incorrectly classified, the predicted class is always class I (uniform behaviour). These rules display sparse, double strip-down lines, while most often the  $32 \times 32$  images extracted for the 200 test observations do not. A different, larger, selected image could reduce the incorrect predictions.

The Normal compression classification (Zenil and Villarreal-Zapata, 2013) splits the 256 rules in two classes,  $C_{1,2}$  and  $C_{3,4}$ . In summary, the rules assigned to class I and II in Wolfram's classification are assigned to class  $C_{1,2}$ , and all rules from Wolfram's class III and IV are assigned to  $C_{3,4}$ . There are a few exceptions: rules 62, 73 and 94 belong to Wolfram's class II, yet are assigned to  $C_{3,4}$ . For this classification, 253 rules of 256 are correctly classified more than 90% of the time. The rules least correctly classified are the rule 94 (50.5%) and the rule 133 (55%), which is equivalent to 94. In contrast, rules 67, 73 and their equivalents are correctly classified more than 97% of the time. The CNN does not know how to classify the rule 94. Nevertheless, this classification accuracy (i.e. the accuracy of the CNN trained with this classification) is very close to Wolfram's CNN accuracy when it uses only two classes, with similar split of rules. We could therefore expect a greater accuracy.

For the Surface Dynamics classification (Seck Tuoh Mora et al., 2014), 255 rules out of 256 are classified correctly more than 90% of the time. No rule stands out in terms of misprediction. Note that this classification uses three classes, versus four in Wolfram's.

Finally, when inspecting how equivalent rules are classified, we notice that the less accurate classifiers (trained for a classification) often incorrectly classify some equivalent rules, while correctly predicting other equivalent rules. The split between mispredicted and correctly predicted equivalent rules does

not follow any equivalence logic, such as visual symmetries.

The classification accuracy results reported may also depend on the capacity of the CNN. The chosen CNN is relatively simple, deeper CNN architectures might be able to capture the logic in the other, less well-learned, classifications. This hypothesis could be tested by performing the same evaluation across a spectrum of CNNs, of increasing capacity.

## 5 CONCLUSIONS

Convolutional neural networks have proven their capability in many applications and in particular for pattern recognition in images. We have used this asset to compare a long list of elementary cellular automata classifications. The experimental results demonstrate the ability of a neural network to learn CA classifications based on logical or abstract concepts, indirectly, via their visual representation. Several classifications (Wolfram, Surface Dynamics, Normalised Compression, Topological) are extremely well captured by this approach (and all are well captured), suggesting that convolutional neural networks could be applied to other areas of the cellular automata domain. For example, we could apply the Wolfram CNN classifier presented here on non-CA output, such as part of the memory of a running program, to observe if the predicted class matches Wolfram's class of ECAs that are thought to be capable of universal computation (Cook, 2004; Martinez et al., 2013) (such as rule 110).

One uncertainty in this method is the choice of the extracted image, from the ECA output, which serves as input data to the neural network. Our experiments show excellent results (prediction accuracy) from very small ECA output extracts, using little training data (100 instances for each CA rule), and with a simple CNN architecture (thus quickly trained). Moreover, the ECA output selection is chosen such that the influence of all 513 cells is accounted for, in order to capture the complex system behaviour of an ECA. Different results could be obtained from a different selection, and more observations.

Also, we provide a sketched proof for a pathological behaviour of two ECA rules, previously unreported (to our best knowledge).

The possibility that deeper CNNs could lead to better accuracy for other classifications is considered future work. This hypothesis, if true, could reflect the complexity of a given classification, and thus defines another comparison method (such as: the size of the CNN that achieves over 99% accuracy).

Finally, the CNN-based approach and its results could be used to discover new ECA classifications.

## ACKNOWLEDGEMENTS

The authors wish to thank Christian Hundt of the Nvidia AI Technology Center Luxembourg, and the ICAART reviewers for their insightful comments.

## REFERENCES

- Bach, E. (2020). <https://commons.wikimedia.org/w/index.php?curid=15015440>. Last accessed 22 July 2020.
- Berto, F. and Tagliabue, J. (2017). Cellular automata. In Zalta, E. N., editor, *The Stanford Encyclopedia of Philosophy*. Metaphysics Research Lab, Stanford University, fall 2017 edition.
- Binder, P. (1993). A phase diagram for elementary cellular automata. *Complex Systems*, 7(3):241.
- Cook, M. (2004). Universality in elementary cellular automata. *Complex systems*, 15(1):1–40.
- de Oliveira, G. M. B., de Oliveira, P. P., and Omar, N. (2000). Guidelines for dynamics-based parameterization of one-dimensional cellular automata rule spaces. *Complexity*, 6(2):63–71.
- He, K., Zhang, X., Ren, S., and Sun, J. (2015). Delving deep into rectifiers: Surpassing human-level performance on imagenet classification. In *Proceedings of the IEEE international conference on computer vision*, pages 1026–1034.
- Krizhevsky, A., Sutskever, I., and Hinton, G. E. (2012). Imagenet classification with deep convolutional neural networks. In *Advances in neural information processing systems*, pages 1097–1105.
- Kunkle, D. R. (2003). *Automatic Classification of One-Dimensional Cellular Automata*. PhD thesis, Citeseer.
- Langton, C. (1990). Computation at the edge of chaos: Phase transition and emergent computation. Technical report, Los Alamos National Lab., NM (USA).
- LeCun, Y., Bengio, Y., et al. (1995). Convolutional networks for images, speech, and time series. *The handbook of brain theory and neural networks*, 3361(10):1995.
- Li, W. and Packard, N. (1990). The structure of the elementary cellular automata rule space. *Complex systems*, 4(3):281–297.
- Martinez, G. J., Seck-Tuoh-Mora, J. C., and Zenil, H. (2013). Computation and universality: class iv versus class iii cellular automata. *arXiv preprint arXiv:1304.1242*.
- Martínez, G. J. (2013). A note on elementary cellular automata classification. In Adamatzky, A., editor, *Journal of Cellular Automata*, volume 8, pages 233–259. Old City Publishing, Greenville, SC 29616, United States.
- Moore, E. and Burks, A. (1970). *Essays on Cellular Automata*. University of Illinois, Urbana.



- Oliveira, G. M., de Oliveira, P. P., and Omar, N. (2001a). Searching for one-dimensional cellular automata in the absence of a priori information. In *European Conference on Artificial Life*, pages 262–271. Springer.
- Oliveira, G. M., Oliveira, P. P. d., and Omar, N. (2001b). Definition and application of a five-parameter characterization of one-dimensional cellular automata rule space. *Artificial life*, 7(3):277–301.
- Russakovsky, O., Deng, J., Su, H., Krause, J., Satheesh, S., Ma, S., Huang, Z., Karpathy, A., Khosla, A., Bernstein, M., et al. (2015). Imagenet large scale visual recognition challenge. *International journal of computer vision*, 115(3):211–252.
- Seck Tuoh Mora, J., Medina, J., Martinez, G. J., and Hernández Romero, N. (2014). Emergence of density dynamics by surface interpolation in elementary cellular automata. *Communications in Nonlinear Science and Numerical Simulations*, 19:941–966.
- Silverman, E. (2019). Convolutional neural networks for cellular automata classification. In *Artificial Life Conference Proceedings*, pages 280–281. MIT Press.
- Von Neumann, J. et al. (1951). The general and logical theory of automata. *1951*, pages 1–41.
- Wolfram, S. (1984). Cellular automata as models of complexity. *Nature*, 311(5985):419–424.
- Wolfram, S. (2002). *A new kind of science*, volume 5. Wolfram media Champaign, IL.
- Wuensche, A., Lesser, M., and Lesser, M. J. (1992). *Global Dynamics of Cellular Automata: An Atlas of Basin of Attraction Fields of One-Dimensional Cellular Automata*, volume 1. Andrew Wuensche.
- Zenil, H. and Villarreal-Zapata, E. (2013). Asymptotic behavior and ratios of complexity in cellular automata. *International Journal of Bifurcation and Chaos*, 23(09):1350159.